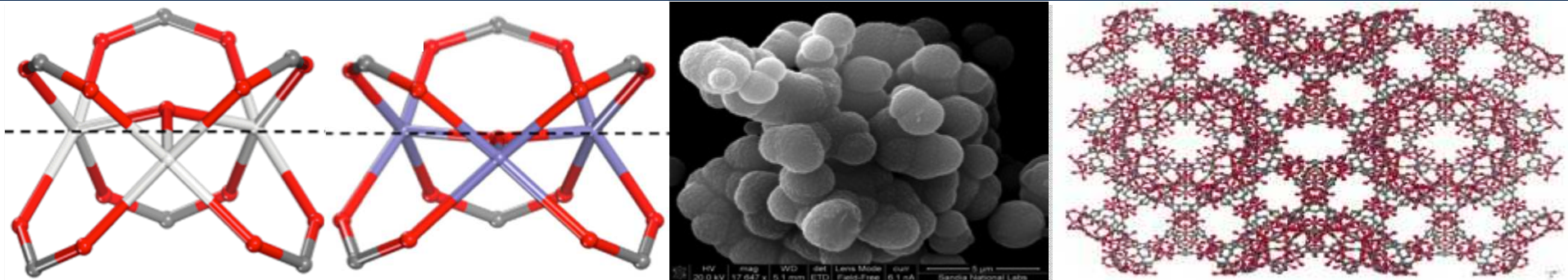


Exceptional service in the national interest



Light Gas Separations with MOFs via Predictive Modeling and Tuned Synthesis

Tina M. Nenoff, Dorina F. Sava Gallis, Marie V. Parkes, Jeffery A. Greathouse, Mark A. Rodriguez, Karena W. Chapman*

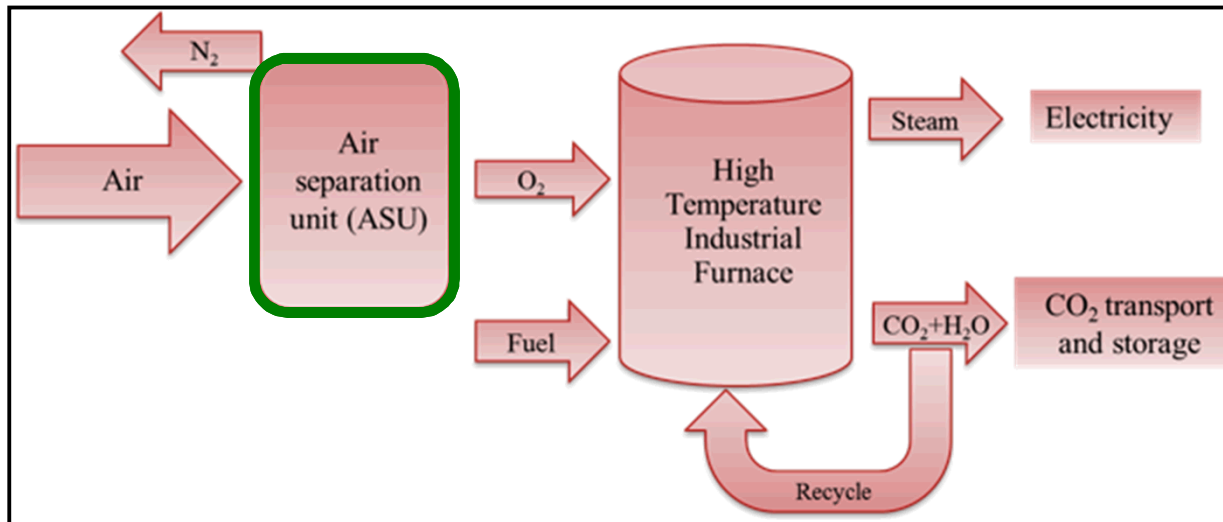
Sandia National Laboratories, Albuquerque NM USA

*Advanced Photon Source, Argonne National Laboratory, Argonne, IL USA

2016 Spring ACS Meeting,
San Diego, CA March 17, 2016

This work is supported by the Laboratory Directed Research and Development Program at Sandia National Laboratories. Sandia National Laboratories is a multi-program laboratory managed and operated by Sandia Corporation, a wholly owned subsidiary of Lockheed Martin Corporation, for the U.S. Department of Energy's National Nuclear Security Administration under contract DE-AC04-94AL85000. Work done at Argonne and use of the Advanced Photon Source, an Office of Science User Facility operated for the U.S. DOE/Office of Science by Argonne National Laboratory, was supported by the US DOE, Contract No. DE-AC02-06CH11357

O_2/N_2 air separations with MOFs to Increase the Efficiency of the *ASU*

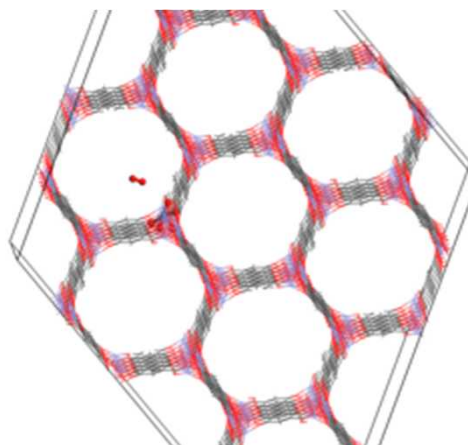
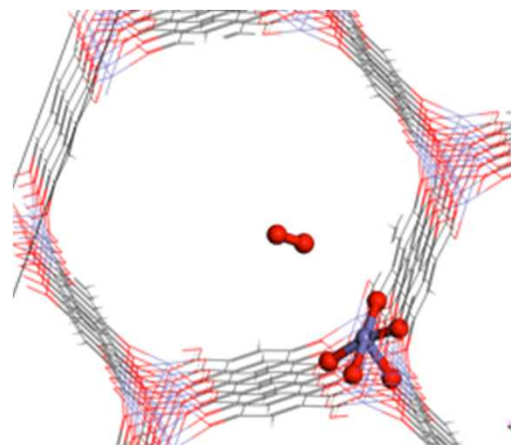
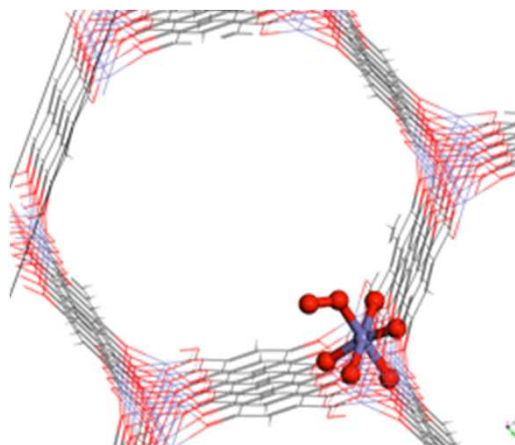


- Oxygen-enriched (oxy-fuel) combustion: burning the fossil fuel in an O₂ rich atmosphere results in a flue gas composed mainly of CO₂ and water (little or no SO_X and NO_X emissions)
- The limiting factor of this technology is the efficiency of the Oxygen Purification Steps: **Cryogenic** ASU, a costly and energy intensive process (primarily compression) for 99+% purity, or **zeolites + PSA** for ~90-95% purity
- Our study is focused on new highly selective materials to increase the efficiency of this separation process

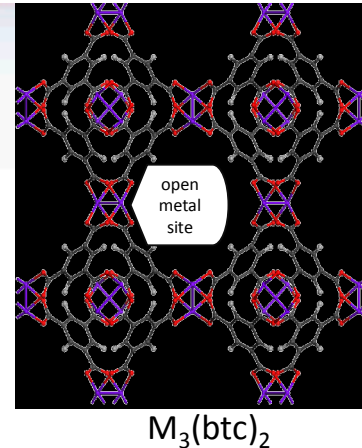
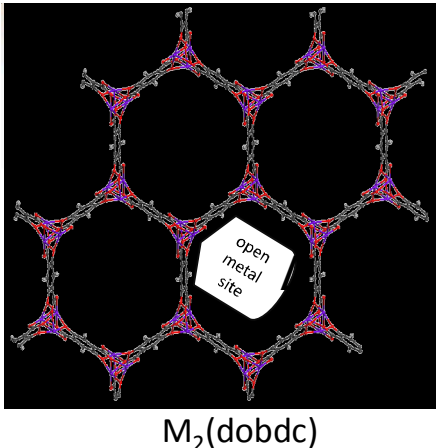
Goal: determine the O₂ and N₂ uptake dependency with temperature
in MOFs with coordinatively unsaturated metal sites

Metal-O₂ and Metal-N₂ Binding Energies and Geometries

- MOFs with coordinatively unsaturated metal centers are promising materials for O₂/N₂ separations
- Two prototypical MOFs from this category, $\text{Cr}_2(\text{BTC})_3$ (*J. Am. Chem. Soc.* **2010**, *132*, 7856–7857) and $\text{Fe}_2(\text{DOBDC})$ (*J. Am. Chem. Soc.* **2011**, *133*, 14814-14822) both show preferential adsorption of O₂ over N₂
- Plane wave DFT calculations were performed on periodic structures in the [Vienna Ab initio Simulation Package \(VASP\)](#)
- Binding geometries for side-on and bent O₂ and bent and linear geometries for N₂ were evaluated
- Static binding energies for O₂ and N₂ at 0 K

MOF with O₂ in poreO₂ ready to bind to metalO₂ bound to metal

DFT modeling of Oxygen Adsorption in Varied Metal-Centered MOFs



MOF metal sites = separate O_2/N_2 by differences in bonding & electronic properties

Plan wave density functional theory (DFT) calculations were performed on periodic structures of each MOF in the Vienna ab initio simulation package (VASP) with the Perdew-Burke-Ernzerhof (PBE) functional including dispersion corrections (DFT-D2). Geometries were optimized and static binding energies ($\Delta E_{\text{O}_2}, \Delta E_{\text{N}_2}$) were calculated by

$$\Delta E_{\text{O}_2} = E_{\text{MOF+O}_2} - E_{\text{MOF}} - E_{\text{O}_2}$$

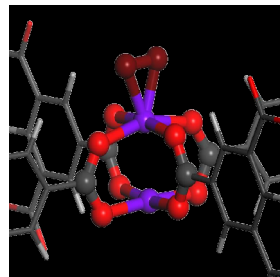
The differences in binding energies ($\Delta\Delta E$) for oxygen and nitrogen were calculated by

$$\Delta\Delta E = -(\Delta E_{\text{O}_2} - \Delta E_{\text{N}_2})$$

Attention Paid to Bonding Geometries

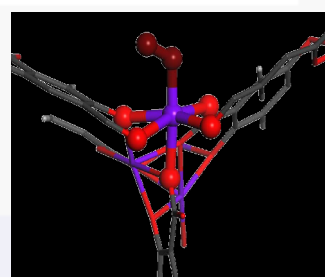
Side-on bonding

$\Delta M\text{-X-X} 67^\circ - 71^\circ$



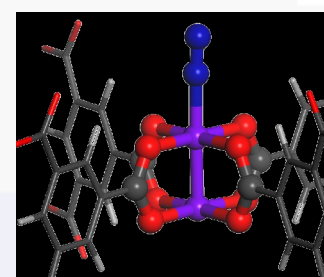
Bent bonding

$\Delta M\text{-X-X} 116^\circ - 159^\circ$



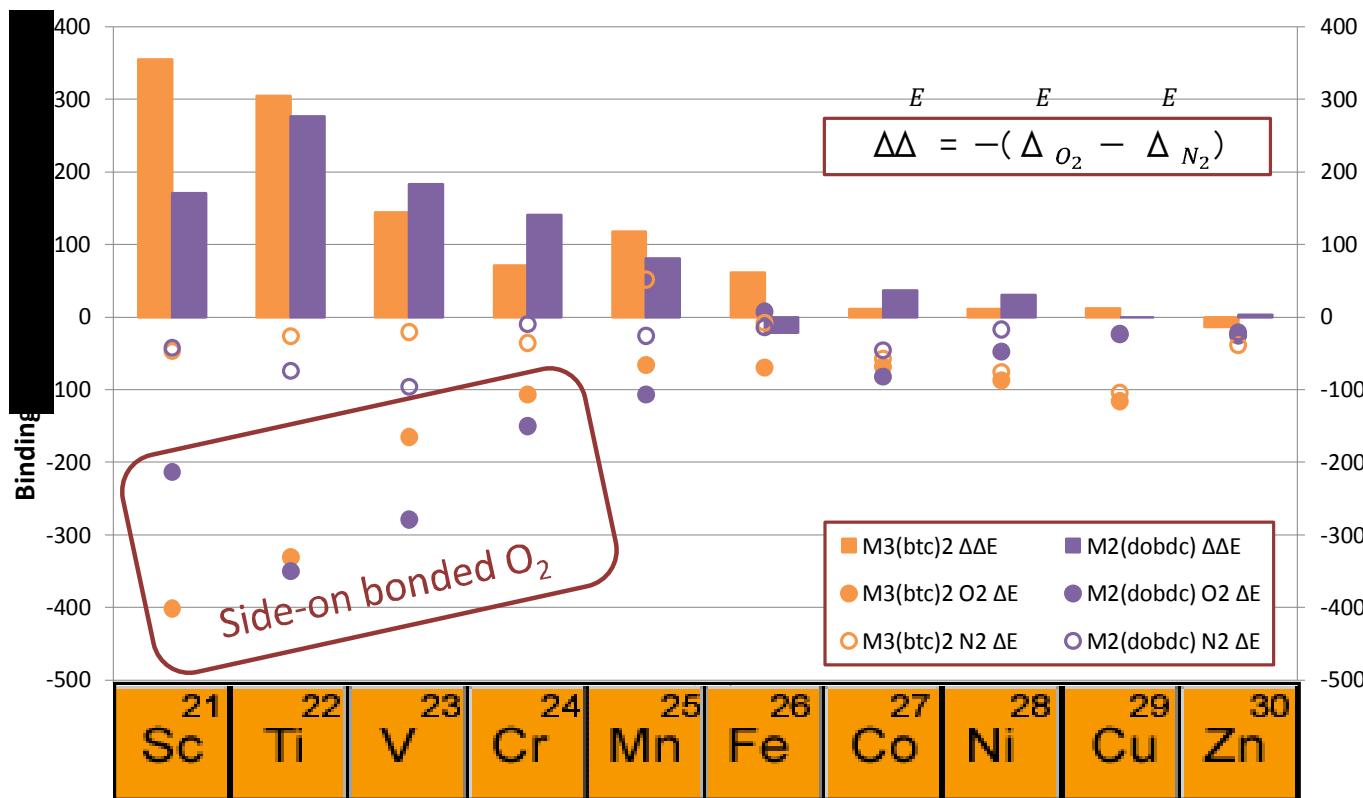
Linear bonding

$\Delta M\text{-X-X} 165^\circ - 179^\circ$



Transition to Quantum Calculations to Estimate Metal-Oxygen Binding Energy

Binding Energy Calculated as a Function of Metal Site



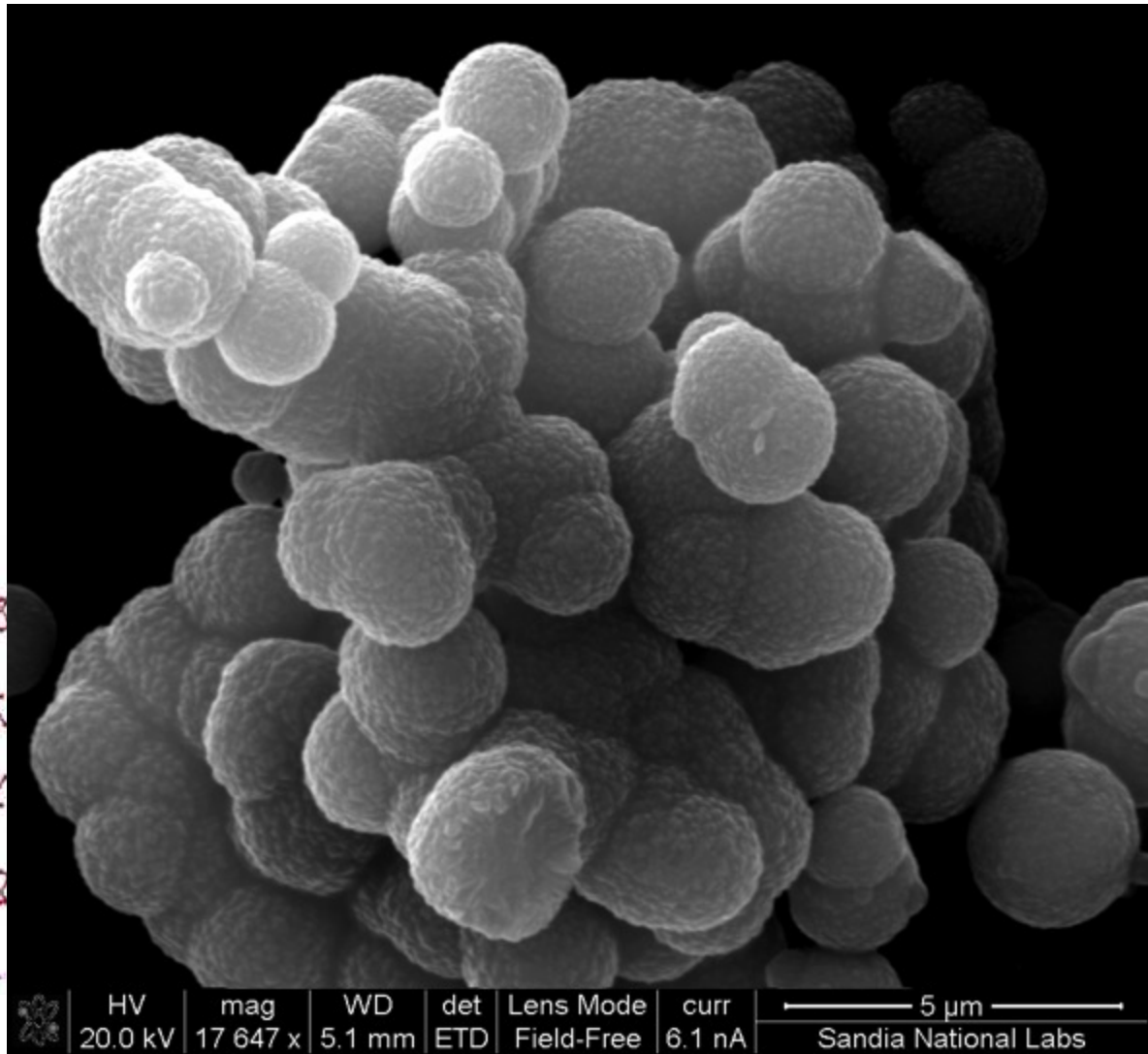
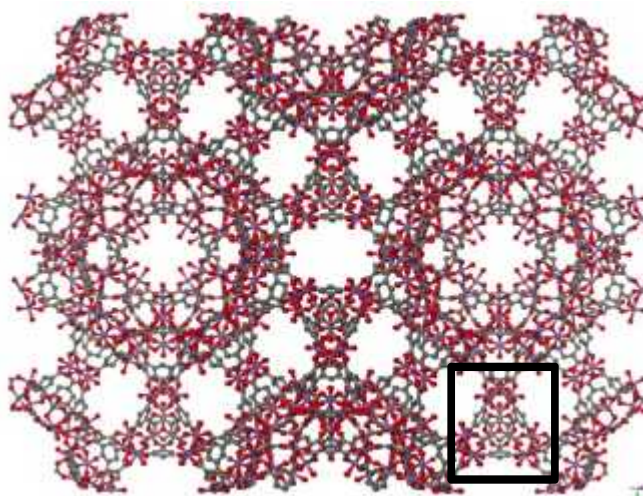
Current Study: Parkes, M.; Sava Gallis, D. F.; Greathouse, J.A.; Nenoff, T.M. "Using Ab Initio Molecular Dynamics to Examine Gas Adsorption on Open Metal Sites of M₂(dobdc)" **2016**, submitted.

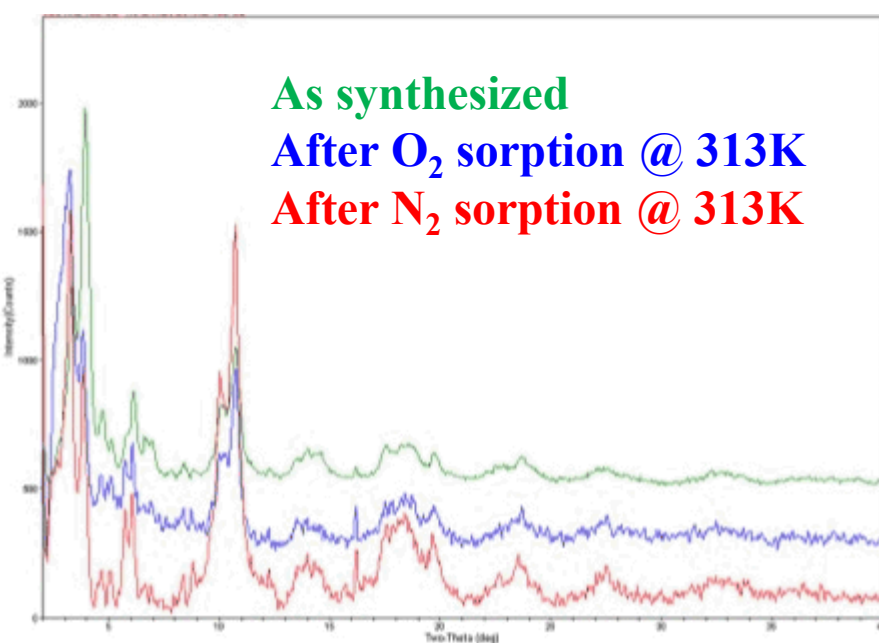
Sc-MIL-100

Unique synthesis:

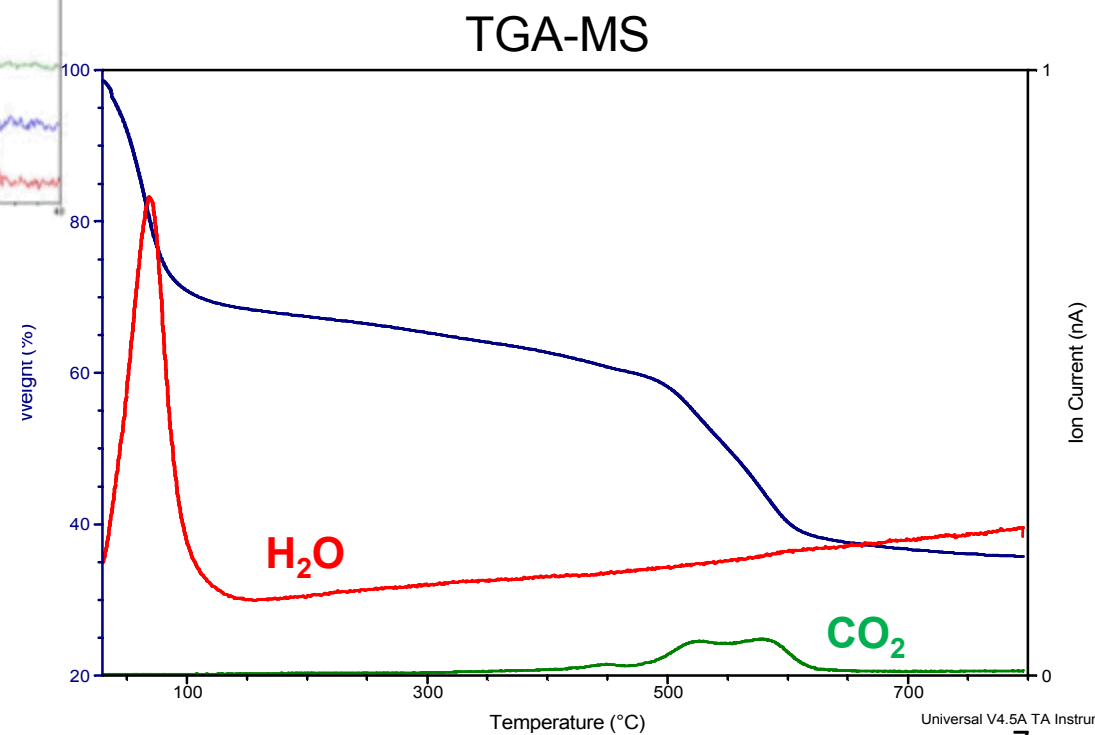
Mixed $\text{Sc}(\text{NO}_3)_3 \cdot x\text{H}_2\text{O}$ and 1,3,5-benzetricarboxylic acid in $\text{N,N}'\text{-dimethylformamide}$ and HCl .

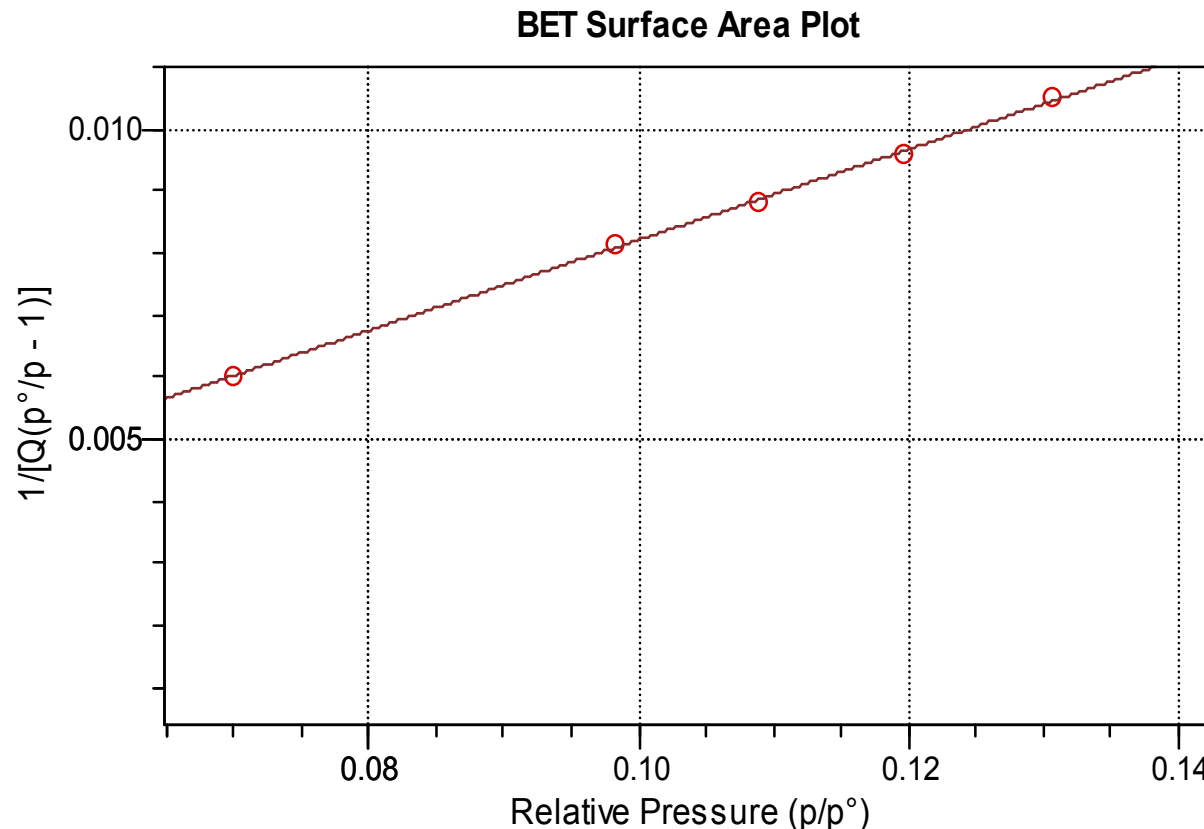
Heated to 373K overnight





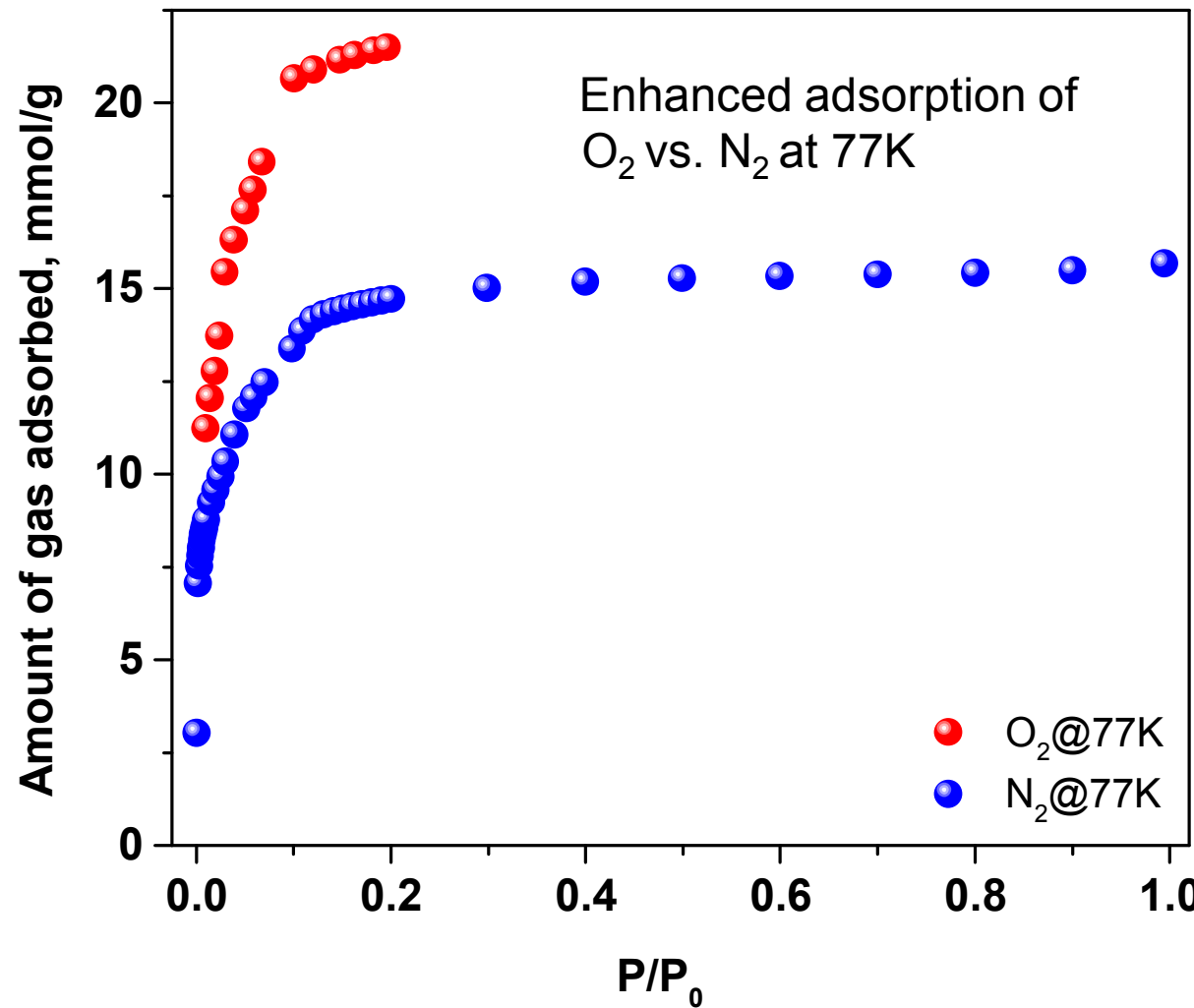
Stable MOF framework over Wide Temperature Range and with Exposure to Variety of Gases





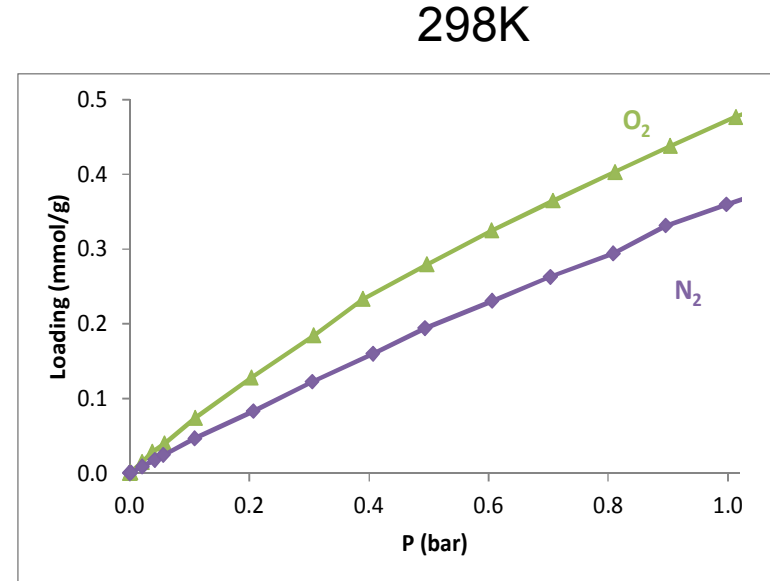
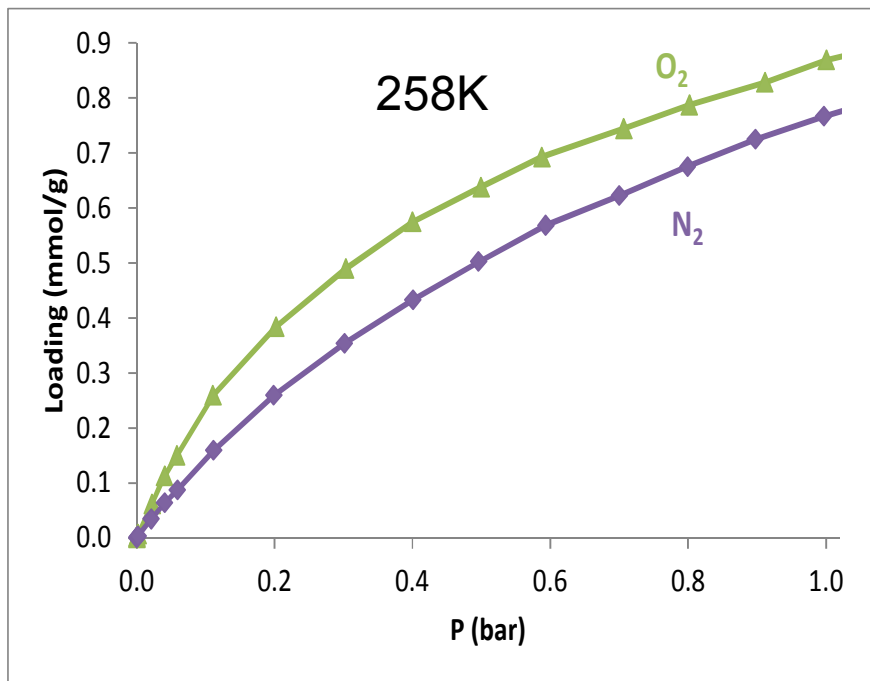
BET surface area: $1321.7194 \pm 24.4623 \text{ m}^2/\text{g}$

Sc-MIL-100: Metal-Center has a role at 77K



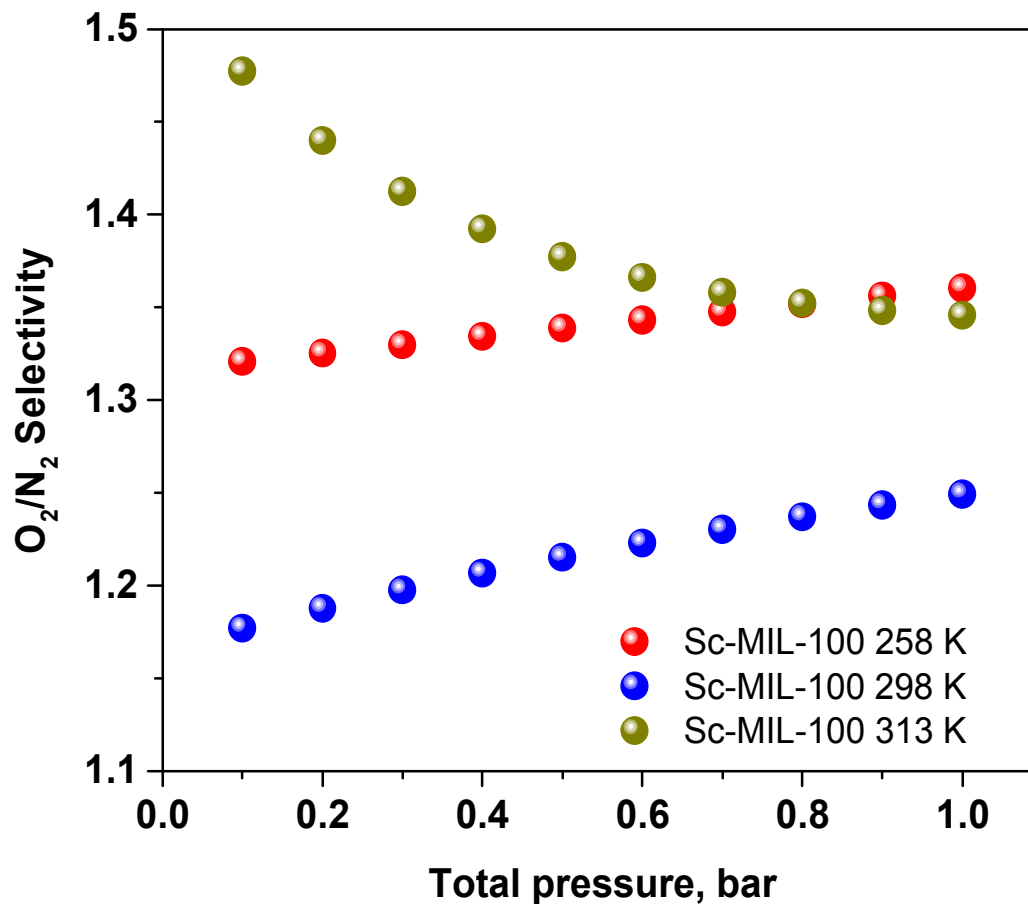
How does Sc-MIL-100 behave at more realistic operational temperatures?

- **Grand Canonical Monte Carlo (GCMC) Simulations**
- Pure gas (N_2 or O_2) adsorption over pressure range 0 - 1 bar.
- Temperature range matched with experiment: 258 K, 298 K, 313 K.
- Grand canonical ensemble (constant chemical potential, temperature, volume) using the Towhee code (Martin, *Mol. Sim.* **2013**, *39*, 1212).
- Gas-gas and MOF-gas interaction energies include van der Waals and electrostatic interactions.
- Framework atoms kept at their crystallographic coordinates.



Preferred O_2 uptake but O_2/N_2 selectivity increases between 258K and 298K

Simulations of Competitive Gas Adsorption: based on GCMC data, 298K

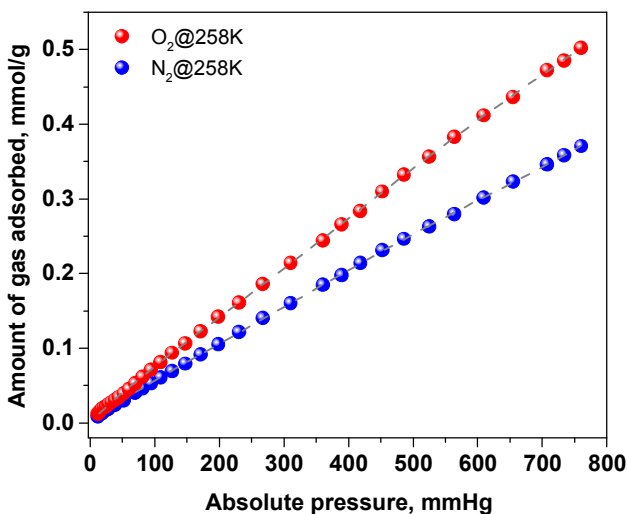


Ideal Adsorbed Solution Theory (IAST) used to calculate mixture adsorption and O_2/N_2 selectivity for **20:80 mixture ($O_2:N_2$)**.

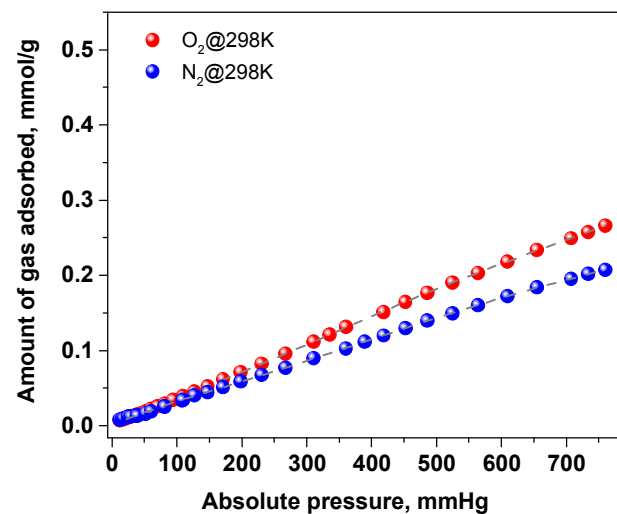
Sc-MIL-100: Enhanced Quantity of O_2 vs N_2 Adsorbed over Wide Temperature Range (at least to 313K)

Fit using the virial eq.

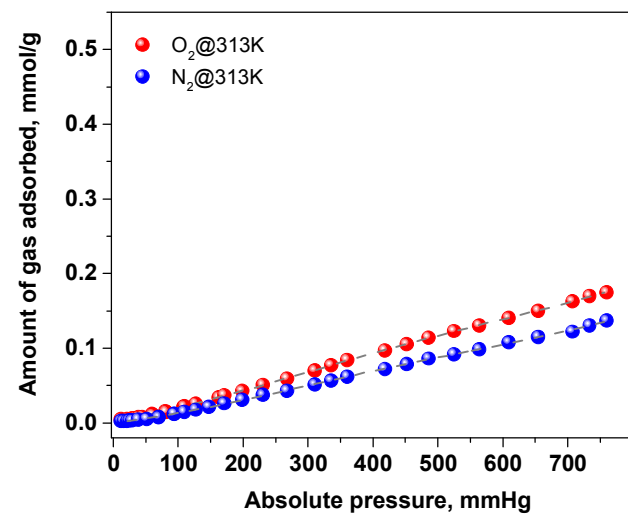
O_2 vs. N_2 @258K



O_2 vs. N_2 @298K



O_2 vs. N_2 @313K

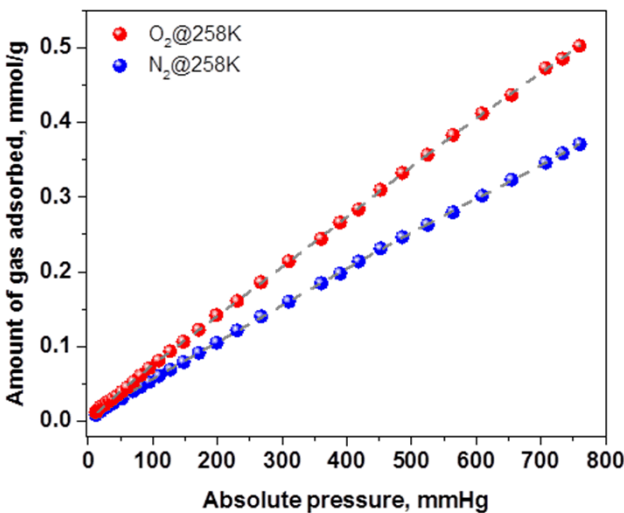


Isotherm trends mimic those predicted by GCMC

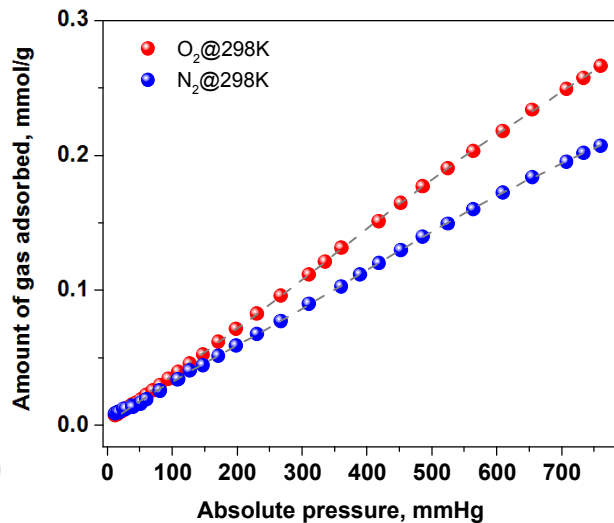
Sc-MIL-100: Enhanced Quantity of O_2 vs N_2 Adsorbed over Wide Temperature Range (at least to 313K)

— Fit using the virial eq.

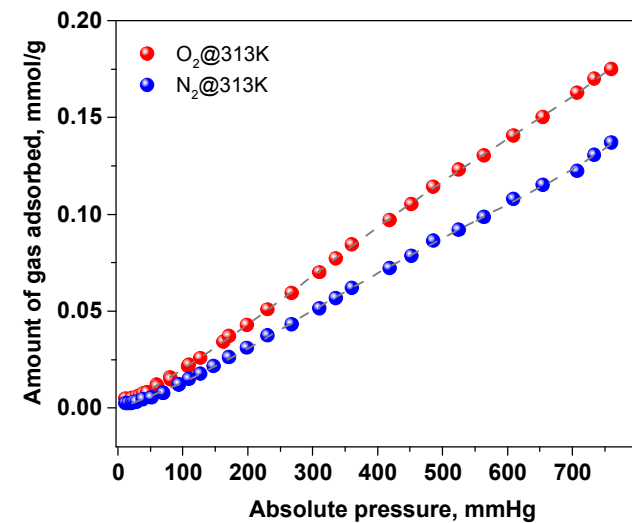
O_2 vs. N_2 @258K



O_2 vs. N_2 @298K



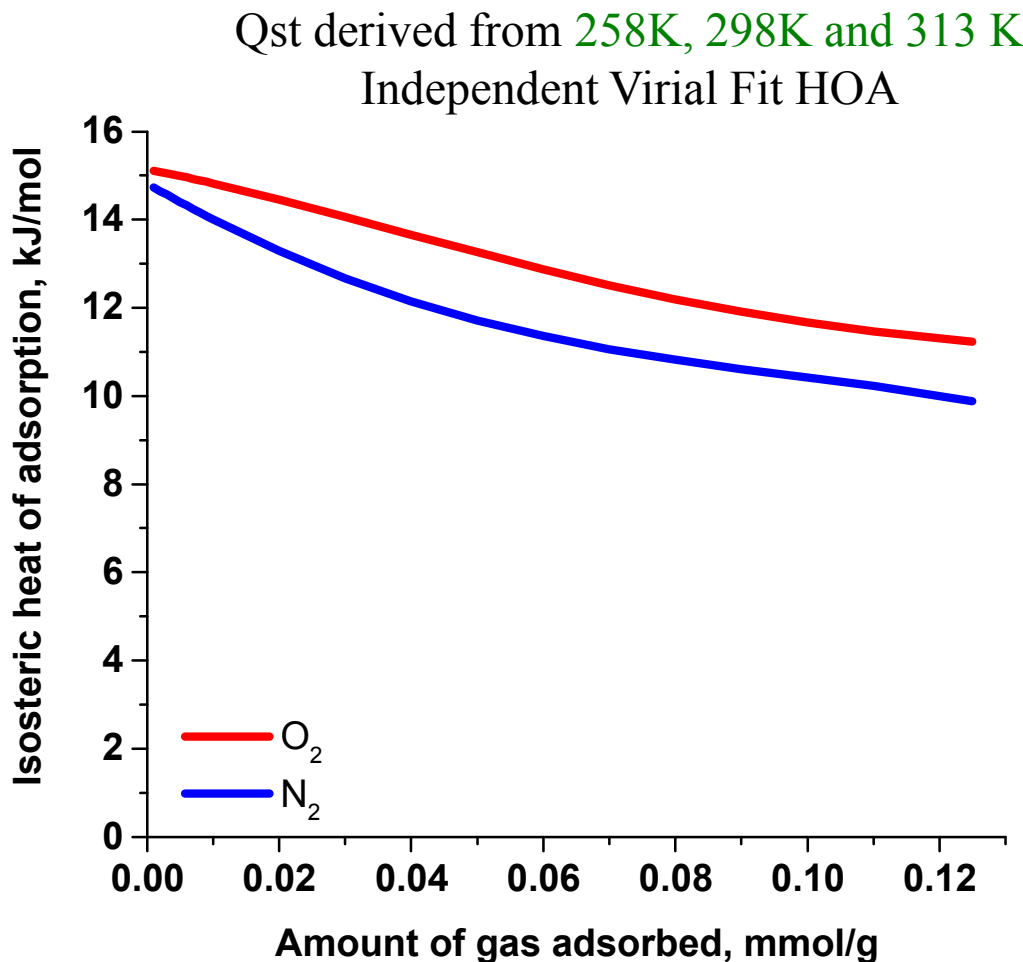
O_2 vs. N_2 @313K



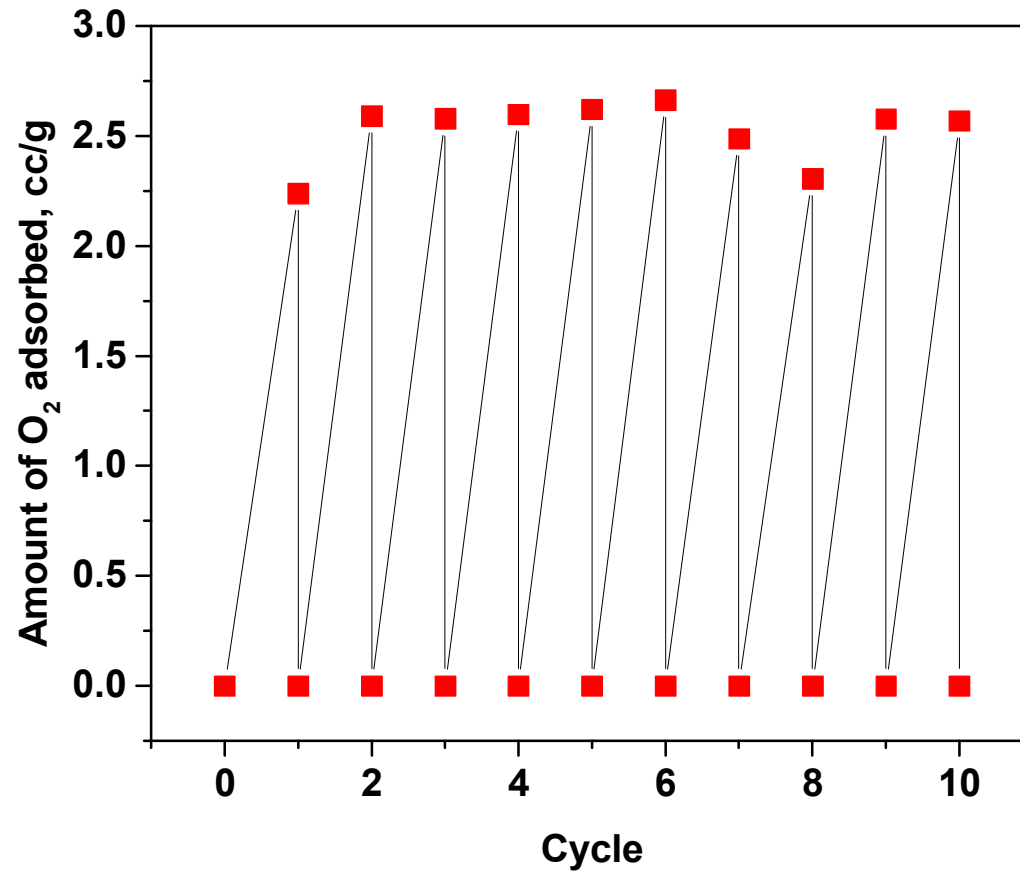
Isotherm trends mimic those predicted by GCMC

Sc-MIL-100: Isosteric Heat of Adsorption (kJ/mol)

Higher Binding Energy in SMOF-8 for O₂ vs N₂



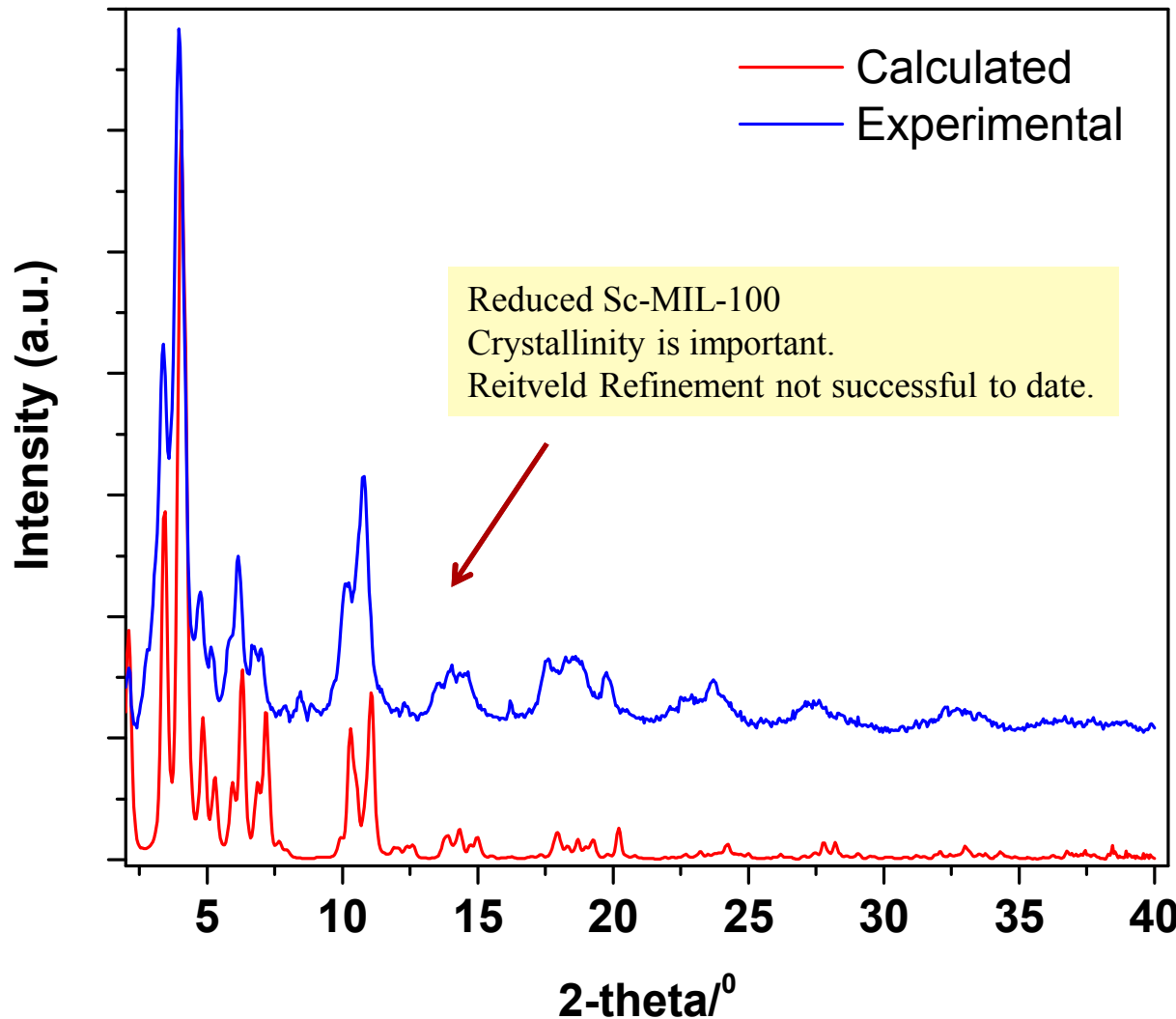
O₂ adsorption and Desorption over 10 cycles, 298 K, 1 atm



What about the structure is making Sc-MIL-100 O₂ strongly sorbing?

Structure-Property Relationship Understanding of Sc-MIL-100 Oxygen Selectivity

High Energy Synchrotron X-ray, APS/ANL



The PDF, $G(r)$, is related to the **probability** of finding an atom at a distance r from a reference atom. It is the Fourier transform of the total structure factor, $S(Q)$.

$$G(r) = 4\pi r \rho_0 [g(r)-1] = (2/\pi) \int Q [S(Q) - 1] \sin(Qr) dQ$$

$\overbrace{\quad \quad \quad}$
 \uparrow
 probability

 $\overbrace{\quad \quad \quad}$
 \uparrow
 structure factor

The structure factor, $S(Q)$, is related to coherent part of the diffraction intensity

$$S(Q) = 1 + \underbrace{[I^{coh}(Q) - \sum c_i |f_i(Q)|^2]}_{\substack{\text{diffraction intensity} \\ \text{(corrected)}}} / |\sum c_i f_i(Q)|^2$$

Apply corrections for background, absorption, Compton & multiple scattering

Use of high energy X-rays and large area detectors key to structure resolution

PDF measurements: APS/ANL Collaboration

Does it matter which synchrotron?

Yes. Only higher energy storage rings produce significant fluxes of high energy X-rays

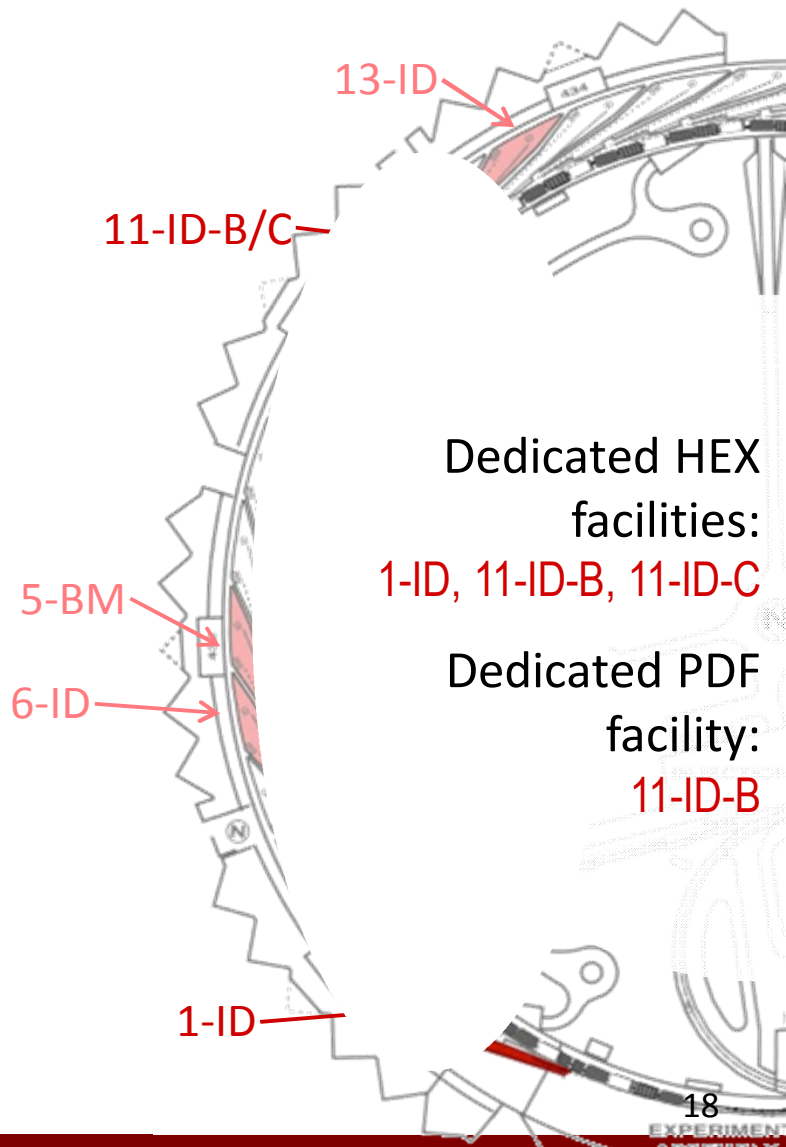
High energy X-rays are a unique strength of the *Advanced Photon Source* (in the western hemisphere)

- 3 dedicated high energy beam lines
- 1 dedicated PDF beamline

APS 11-ID-B: Dedicated PDF facility
 - 58 or 90KeV high energy X-rays
 - typical wavelengths = 0.1 - 0.2Å

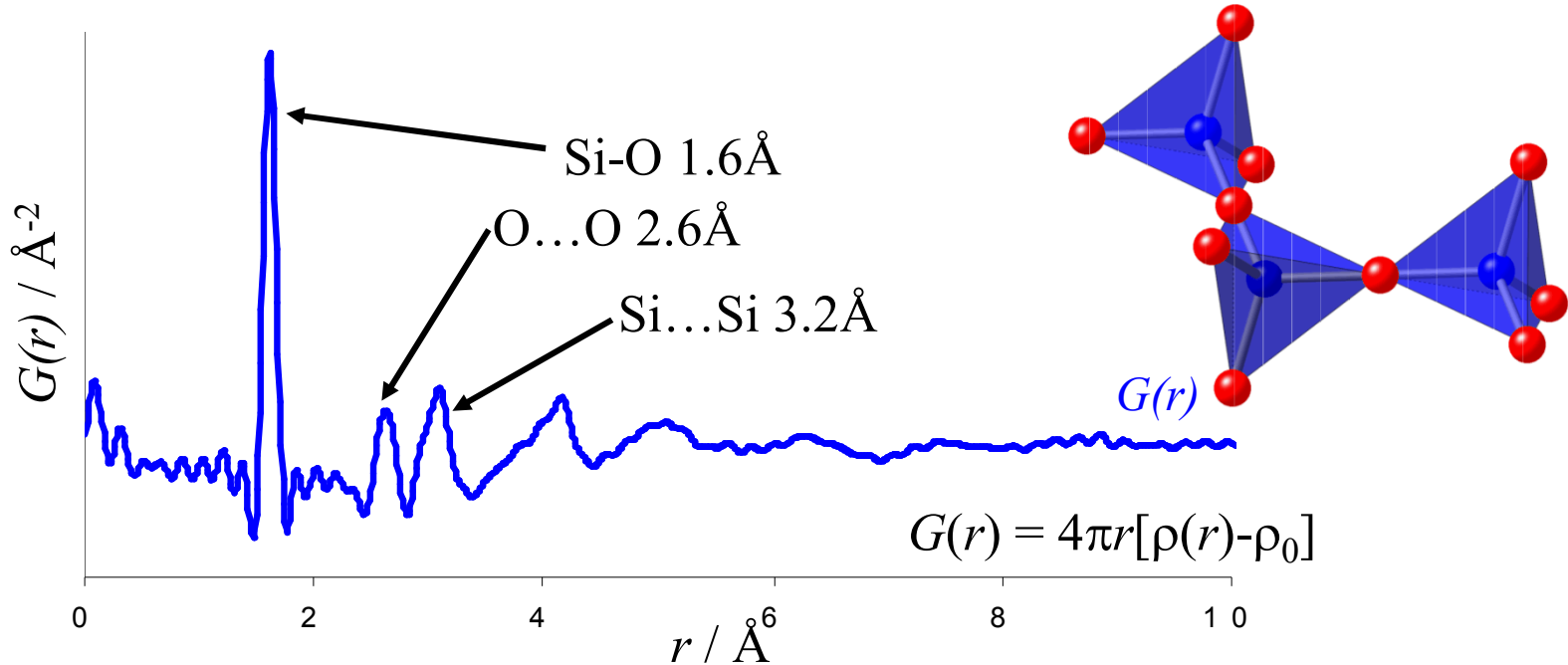
For our experiments:

$Q > 20\text{\AA}^{-1}$; CuK_α to $2\Theta = 180$ results in $Q_{\text{max}} = 8\text{\AA}^{-1}$



PDF: Insight Into Short Range Structural Order eg., Amorphous SiO₂ (Glass)

- a weighted histogram of ALL atom-atom distances

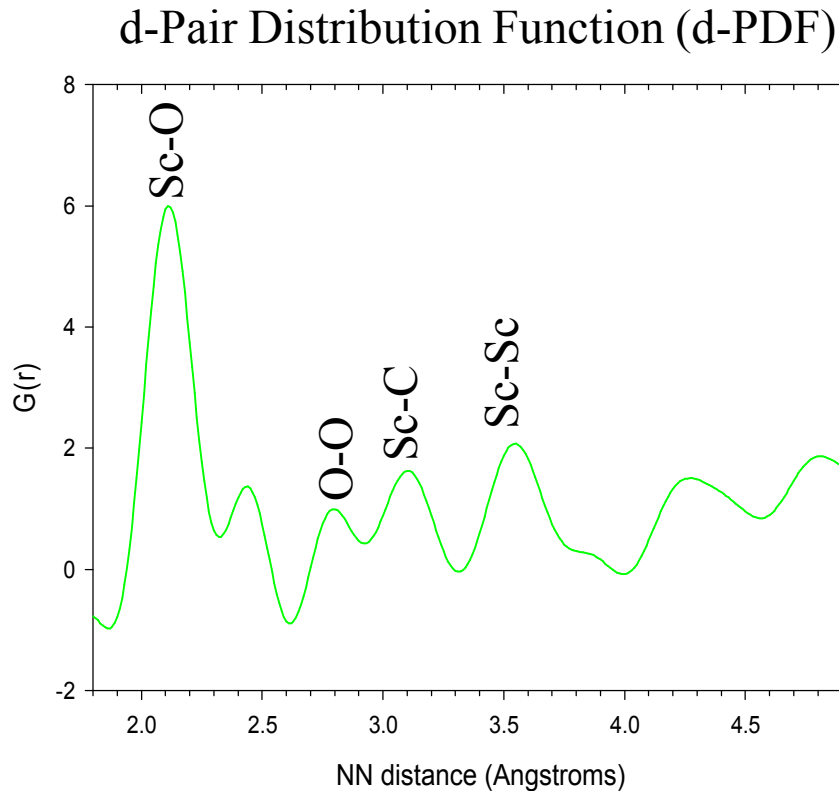


Peak position → Bond length / distance
 Peak area → Coordination #, scattering intensity
 Peak width → Disorder, bond angle distribution
 Peak r_{max} → Particle size, coherence

Structural Modeling

Application to Nanoporous Materials to Examine Short Range Interactions

Sc-MIL-100: Structure-Property relationship evaluated.



Peaks shifted to longer distances
Consistent with larger Sc incorporation
(vs. Cr-MIL-100)

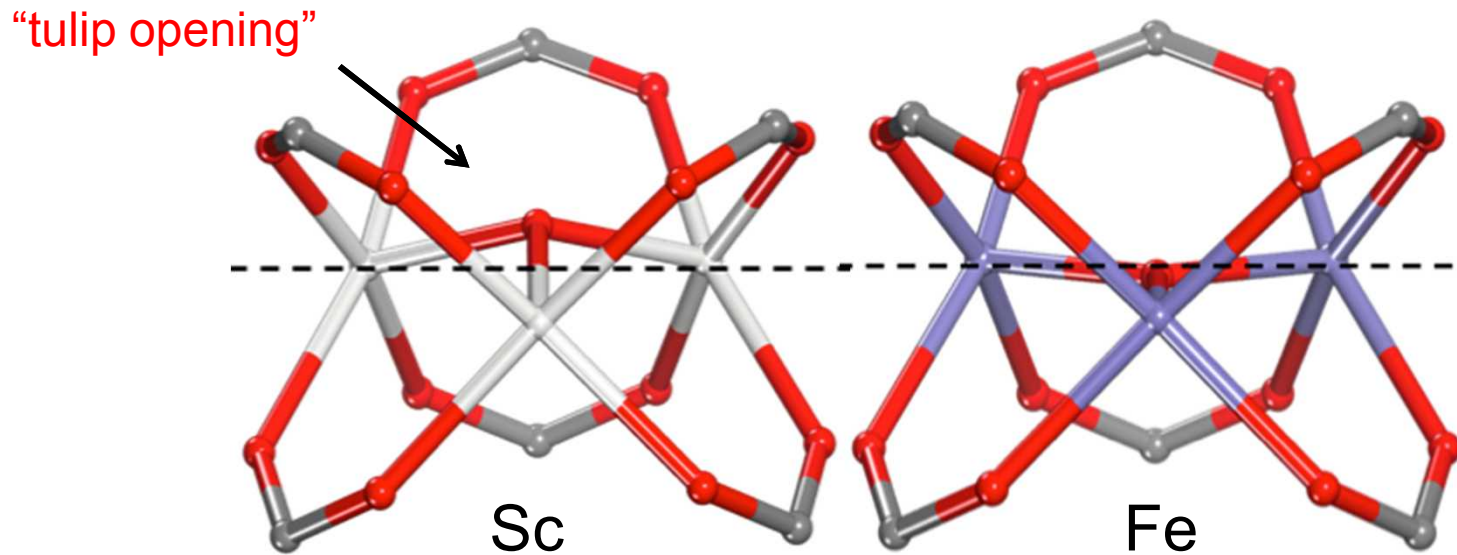
d-PDF peak analysis

Bond	NN distance (Å)	Area	FWHM (Å)
Sc-O	2.11	1.5	0.19
O-O	2.81	0.3	0.22
Sc-C	3.08	0.8	0.26
Sc-Sc	3.53	0.5	0.24

- Oxo-centered trimers at nodes of MIL-100 framework inferred from M-O and M...M distances
- Narrow Sc-O peak = narrow Distribution of bond lengths
- Single M-O bond length ($M-O(\mu_3)$ or $M-O$ (carboxylate)), suggests **M-O-M angle of 113°**
 $\ll 120^\circ$ of a planer trimer

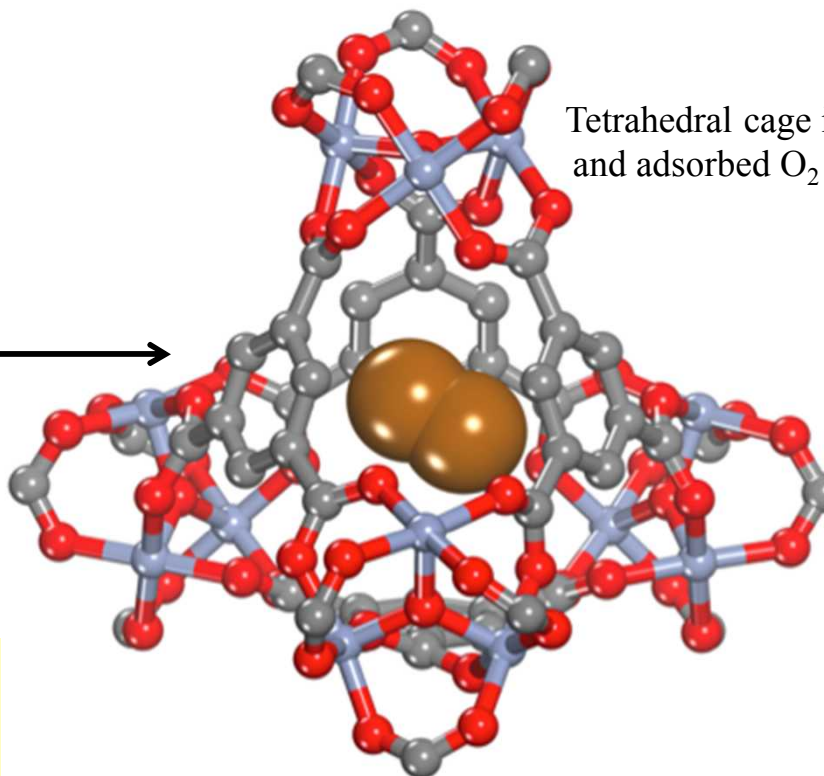
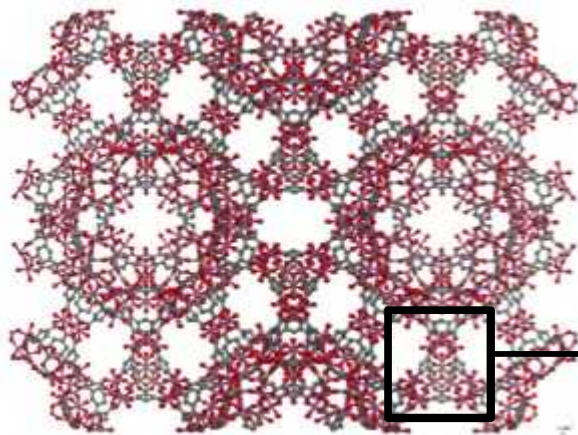
Sc-MIL-100: Structure-Property relationship evaluated. Preferred O₂ sorption – Large Sc Distorts Cluster

Large size of Sc atom requires **out of plane distortion** in the ozo trimer of the O(μ 3) atom.
Resultant “**puckering**” of trimer and “bending” of ligand is
probable route for enhanced O₂ sorption / insertion in Sc-MIL-100



Rietveld refinement unit cell for Sc-MIL-100: $a = 74.518(31)$ Å, $R = 10.7\%$

Sc-MIL-100: Probable Sc-O binding sites



Tetrahedral cage in the MIL-100 framework and adsorbed O₂ molecule (large spheres).

GCMC-equilibrated configurations:

Cage and pore occupancy
as determined at 298K and 1 bar

P (bar)	Gas	# in Cage	# in Pore	Total
1	N ₂	21	27	48
1	O ₂	47	20	67

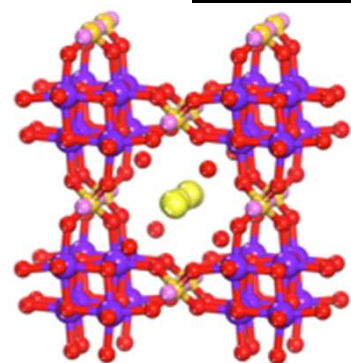
Conclusions and future work

- Successfully synthesized partially substituted Co-, Fe- and Mn- analogues of Cu-BTC
- Assessed the effect on metal substitution on the O₂ and N₂ adsorption capacity at both cryogenic and close to room temperature ranges
- For the Co-, Mn- and original Cu-BTC, O₂ preferentially adsorbs over N₂ at 77K. **However**, the trend is reversed at 298K, where N₂ preferentially adsorbs over O₂
- Based on predictive modeling, we studied early transition metal metal-center MOFs for enhanced O₂ sorption.
- **Sc-MIL-100**: Early transition metal MOFs show preference for O₂ vs N₂ over wide temperature range (up to at least 313K), as confirmed by isosteric heats of adsorption.
- **On-going Steps**: Data transfer to *Technoeconomic Analysis* and *Burner Design* for Oxyfuel combustion applications; higher TRL testing

Extra slides



Novel SNL Separations and Waste Forms: Technologies for Environment and Energy Applications



R&D100 1996

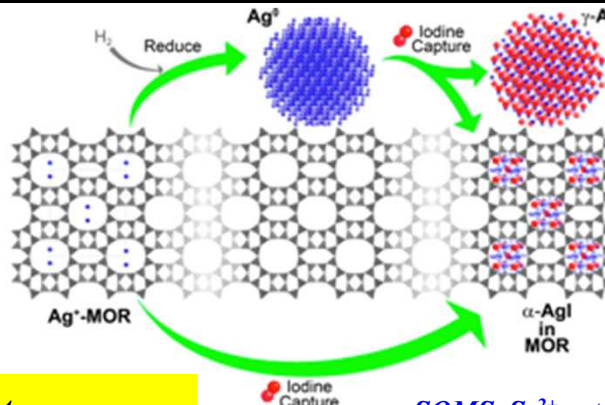
JACerS, 2009, 92(9), 2144

JACerS, 2011, 94(9), 3053

Solvent Extr. & Ion Exch, 2012, 30, 33

CST, Cs⁺ removal from water to Pollucite Waste Form

US Patents 6,479,427; 6,110,378

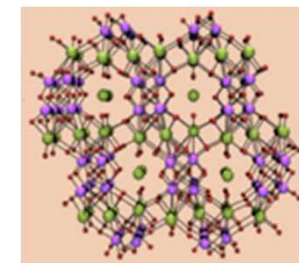


Ag-MOR

I₂(g) capture & mechanisms

JACS, 2010, 132(26), 8897

J Phys Chem Letters, 2011, 2, 2742



SOMS, Sr²⁺ getter,

1-step to Perovskite WF

JACS, 2002, 124(3), 1704

US Patent 7,122,164

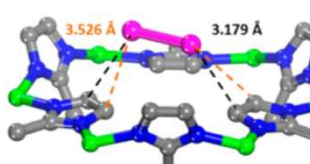
I₂/ZIF-8, Isolation to Waste Form

JACS, 2011, 133(32), 12398

US Patent filed 2012

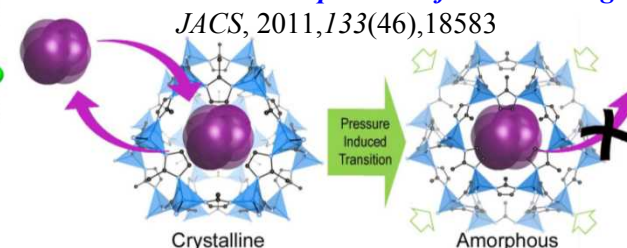
JACS 2013, 135, 16256

Fundamental Research to Applied to Commercial Products
Design the Separation Material To Develop the Waste Form



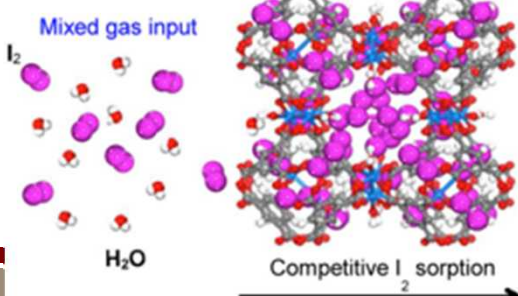
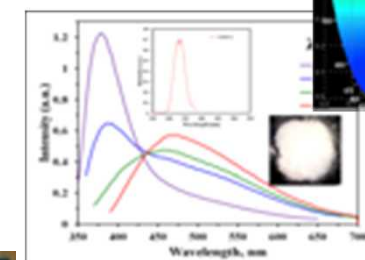
MOF Amorphization for Gas Storage

JACS, 2011, 133(46), 18583



MOFs
White Light PL

JACS, 2012, 134 (9), 3983



Cu-BTC: I₂ from Humid Gas Stream
Chem. Mater. 2013, 25(13), 2591

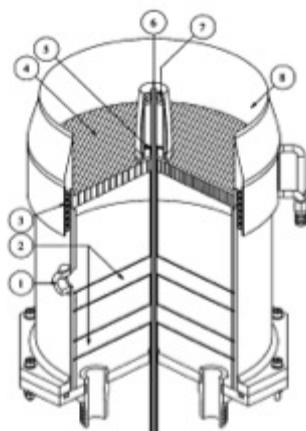


Binder Free MOF Pelletization

US Patent 2015 9,117,560

Universal Core-Shell Iodine Glass Waste Form & Getter
JACerS, 2011, 94(8), 2412
US Patent 8,262,950; 2012

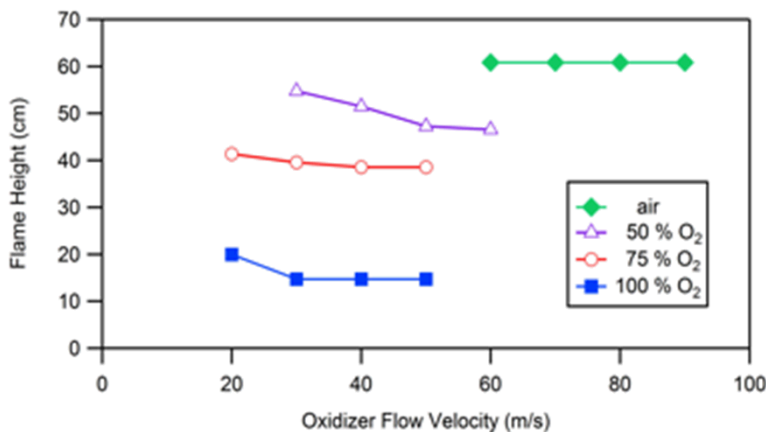
Coupling of Burner design and Oxy-fuel Combustion to Radiant Heat Transfer



Callout number	Description
1	Flashback over-pressure sensing port
2	Outer burner tube
3	Coarse perforated baseplate
4	Coarse perforated baseplate
5	Pilon nozzle feed port
6	Central jet exit
7	Pilon perforated baseplate
8	Coarse center



- Newly designed and constructed burner with smaller diameter inside tube for CH₄ into oxider jet flow
- Allows either premixed or non-premixed methane-air flame
- Designed specifically for pure O₂ and enriched O₂ stream as determined by gas separations data from MOFs and economic life cycle analyses



LDRD calculated/predicted flame heights when using a 1/8", 0.020 wall stainless steel tube to deliver methane to the Dunn burner.

The volumetric flow of methane is always equal to $\frac{1}{2}$ the flow of oxygen, to maintain stoichiometric combustion conditions.

Preliminary Investigation of Oxygen-Enriched NG Flames

Performed preliminary testing performed with oxidizers of pure oxygen and with 50% O₂ in N₂, using an overall equivalence ratio of 1, with a constant methane flow

- Velocity (Re) of oxidizer flow is 50% lower when using pure O₂, making for taller flame (slower mixing)
- Soot formation is enhanced when using pure O₂ (higher temperatures, slower mixing)



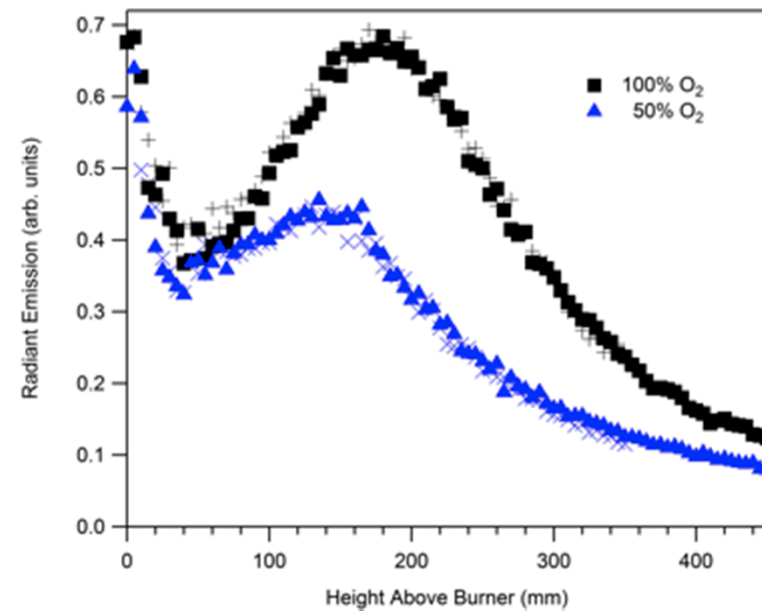
50% O₂ in N₂



100% O₂

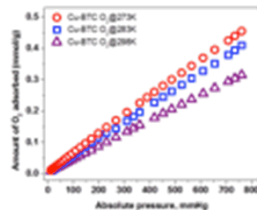
Radiant emission measurements have been performed along the flame centerline

- Data for 100% O₂ shows significantly more thermal radiation
- Flame temperatures are higher when using pure O₂ (more radiation from flame products)
- Some soot is formed in the 100% O₂ flame



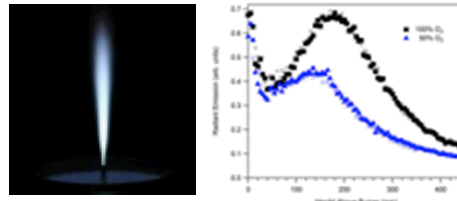
Systems Analysis of MOF-based Air Separation

MOF adsorption isotherms (N_2 & O_2) (from MOF team)



Construct and validate model of PSA process

Optimal O₂:N₂ ratio for combustion (from combustion team)



Can MOF-based
PSA reduce energy
consumption by 5%
vs. conventional PSA
air separation?

- Vessel dimensions
- Operating pressures
- Cycle time
- Feed rate

PSA energy consumption is dominated by compressor(s)
→ Operating pressures and flow rates are primary drivers